

偏光による反射成分の分離および反射パラメータの決定

高橋 徹[†] 佐藤洋一[‡] 池内克史[‡]

[†] 東京大学大学院 理学系研究科

[‡] 東京大学生産技術研究所

〒 106-8558 東京都港区六本木 7-22-1

E-mail : {toru, ysato, ki}@cvl.iis.u-tokyo.ac.jp

あらまし 本研究では、現実中存在する物体から仮想モデルを作成する際に、物体の反射特性を適切に再現する手法について述べる。まず、偏光光源下で物体を偏光板を通して撮影することにより、表面反射成分と内部反射成分を分離する。その後、各反射成分ごとに、Torrance-Sparrow の反射モデルにたいしてフィッティングをすることにより、反射モデルのパラメータを決定する。パラメータ決定の際、幾何的情報については、レンジセンサーによって得られた距離画像をもとにつくられた3次元メッシュモデルを利用する。最後に、得られたパラメータをもとに、物体の仮想画像を合成する。

Separating the reflection components with the use of polarization and Determining the reflection parameters

Toru Takahashi[†] Yoichi Sato[‡] and Katsushi Ikeuchi[‡]

[†] Graduate School of Science, The University of Tokyo

[‡] Institute of Industrial Science, The University of Tokyo

7-22-1 Roppongi, Minato-ku, Tokyo JAPAN 106-8558

E-mail : {toru, ysato, ki}@cvl.iis.u-tokyo.ac.jp

Abstract In this work, we propose a new method for reproducing the reflection properties of the objects. First, we separate the reflection components by taking the images of a dielectric object through polarization filter under linearly polarized illumination. Second, for each separated reflection component, we determine the parameters of a reflection model(Torrance-Sparrow). In estimating the parameters, we use 3D mesh-model which is made from range images taken by a range sensor. Last, we synthesize the virtual image using the obtained reflection parameters.

1 Introduction

It becomes more and more important to develop the easy method for getting the accurate reflectance information as the interest in virtual reality is growing. Currently, virtual reality system is used in a wide variety of applications including electronic commerce, simulation-and-training, and virtual museum walk-throughs. In spite of these many needs for virtual reality models, most of the virtual reality systems utilize models that are manually created by programmers. If we can build a system that automatically create the models for virtual reality system, we can drastically decrease modeling costs for virtual reality systems.

When we make a model of reflectance properties by observing real objects, we need to consider two reflection components: the specular reflection component and the diffuse reflection component. If we only map the observed image onto the object shape model as observed surface texture, we cannot reproduce the appearance of the object under different viewing and illumination conditions correctly. When highlights are observed in the original images, those highlights are fixed on a certain position of the object surface permanently regardless of illumination and viewing conditions. Therefore, in order to model the reflection properties correctly, we have to separate the specular reflection and diffuse reflection.

Several techniques to separate the reflection components have been developed. One major approach to the problem is the one that uses color as a clue. Most of color based methods are based on the dichromatic reflection model proposed by Shafer [7]. The dichromatic reflection model suggests that reflected lights from dielectric material have different spectral distributions between the specular and the diffuse reflection components. The specular component has a similar spectral distribution to that of the illumination. On the other hand, the diffuse component has an altered distribution by the colorants in the surface medium. Consequently, the color of an image point can be viewed as the sum of two vectors with different directions in color space. Klinker et al.[8] ob-

served that color histogram of a uniformly colored object surface makes the shape of *skewed T* with two limbs in the color space. One limb represents the purely diffuse points while the other represents highlight regions. Based on this observation, Klinker et al.[8] proposed an algorithm for automatically identifying the two limbs and using them to separate the diffuse and specular reflection components at each surface point. Sato and Ikeuchi [2] used a sequence of color images taken under actively varying light direction, and successfully separated the reflection components for each object surface point even if object surface is not uniformly colored.

Nayer et al. [6] used not only color but also polarization to separate the reflection components. Their proposed algorithm used the partial polarization included in the reflection in order to determine the color of specular component independently for each image point. The specular color imposes constraints on the color of the diffuse component and the neighboring diffuse colors that satisfy these constraints are used to estimate the diffuse color vector for each image point.

All of these separation methods based on the dichromatic reflection model suffers from the common weakness in that they cannot work if the specular and diffuse reflection vectors have same direction in a color space. In this paper, we propose a new method for separating the reflection components using polarization. Unlike the previously proposed methods, our method does not require that the diffuse color and the specular color are different. In order to separate the reflection components in a robust manner, we use a controlled illumination which is linearly polarized, and we take the images of an object through a polarization filter. Our method is able to separate the diffuse and specular reflection components for each image pixel independently, and therefore, it can be applied to objects with complicated surface textures.

2 Reflection Mechanism

A number of reflectance models have been proposed in the past by the researchers in the fields of applied physics and computer vision. In general, these models are classified into two categories: a specular reflectance model and a diffuse reflectance model.

A diffuse reflectance model represents reflected rays resulted from internal scattering inside surface medium. The rays penetrate the surface and encounter microscopic inhomogeneities in the surface. The rays are repeatedly reflected and some of the rays are re-emitted to the surface with a variety of directions.

A specular reflectance model, on the other hand, represents light rays reflected on the surface of the object. The surface may be assumed to be composed of microscopic planar elements, each of which has its own surface orientation different from the macroscopic local orientation of the surface. The result is the specular reflection component that spreads around the specular direction and that depends on the surface roughness for the width of the distribution.

In this paper, the Torrance-Sparrow model is used for representing the diffuse and specular components.

$$I_m = I_{D,m} \cos \theta_i + I_{S,m} \frac{1}{\cos \theta_r} e^{-\alpha^2/2\sigma^2} m = R, G, B \quad (1)$$

where θ_i is the angle between the surface normal and the light source direction, θ_r is the angle between the surface normal and the viewing direction, α is the angle between the surface normal and the bisector of the light source direction and the viewing direction, $I_{D,m}$ and $I_{S,m}$ are the scaling factor for the diffuse and specular components, and σ is the standard deviation of a facet slope of the Torrance-Sparrow model.

In this model, the reflections bounced only once from the light source are considered. Therefore, this model is valid only for the convex objects. So, in this research, we use the objects for which inter-reflection does not affect our analysis significantly.

We refer to $I_{D,m}$ as the diffuse reflection parameters, and $I_{S,m}$ and σ as the specular reflection parameters.

3 Polarization

Polarization has been used for several decades in the remote sensing research. Wolff and Boulton [4] have proposed an algorithm which analyzes linear polarization states of highlights removal and material classification. Boulton and Wolff [5] have also studied the classification of scene edges based on their polarization characteristics. Recently, Saito et al. [10] have proposed a method for measuring surface orientation of a transparent object using the degree of linear polarization in highlights observed on the object.

The method presented in this paper uses two linear polarization filters. One is placed in front of a point light source in order to polarize the light source linearly, and the other is placed in front of a camera to capture images through the linear polarization filter.

For an ideal filter, a light wave should be passed unattenuated when its electric field is aligned with the polarization axis of the filter, and the energy is attenuated as a trigonometric function when the filter is rotated.

As described in the previous section, the image brightness value taken by sensor is described as:

$$I = I_d + I_s \quad (2)$$

where I_d represents the diffuse component and I_s represents the specular component.

When incident light is linearly polarized, the diffuse component tends to be unpolarized due to its internal scattering. In contrast, the specular reflection component tends to remain linearly polarized. Therefore, the observed brightness of the specular component can be expressed as a trigonometric function for polarization filter angle, and that of the diffuse component can be expressed as a constant. Thus the image brightness observed through a linear polarization filter is described as:

$$I = I_c + I_v(1 + \cos 2(\theta - \beta)) \quad (3)$$

where θ is the angle of the polarization filter and β is the phase angle determined by the projection of the surface normal onto the plane of the filter.

It should be noted that in the above equation I_c is not equal to the real diffuse intensity, and $2 \times I_v$ is not equal to the real specular intensity. Both of specular and diffuse components are attenuated traveling through the polarization filter and image brightness gets darker overall the object surface.

The polarization state of reflected light depends on several factors including the material of the reflecting surface element, and the type of reflection component, i.e. diffuse or specular. In order to describe the state of polarization of the reflected light, the Fresnel reflection coefficients $F_{\perp}(\eta, \psi)$ and $F_{\parallel}(\eta, \psi)$ are used[4]. The Fresnel reflection coefficients determine the polarization of reflected light waves in the directions perpendicular and parallel to the plane of incidence, respectively, and determine the maximum and the minimum intensities which are observed when the angle θ of the polarization filter varies. The parameter η is the complex index of refraction of the surface medium and the parameter ψ is the incidence angle. Since we use a linearly polarized light source, we can assume that the intensity of the specular component observed through a linear polarization filter is guaranteed to become equal to zero at a certain angle. Hence, we obtain the following relation between I_v and specular reflection intensity:

$$q = \frac{F_{\perp}(\eta, \psi)}{F_{\parallel}(\eta, \psi)} \quad (4)$$

$$2I_v = \frac{q}{1+q} I_s \quad (5)$$

where I_s equals the specular reflection intensity.

It is known that the diffuse component is also polarized when the viewing angle is close to 90 degrees, e.g., near the occluding contour of an object. However, the diffuse component becomes linearly polarized only in narrow region and the degree of polarization in the diffuse reflection component is generally negligible. Hence, we assume that the diffuse component is unpolarized in our analysis.

The intensity of unpolarized light is attenuated by half when it passes a linear polarization filter. As a result, I_c and the diffuse component have a relation as below:

$$I_c = \frac{1}{2} I_d \quad (6)$$

where $\frac{1}{2} I_d$ is the intensity of the diffuse reflection.

Figure 1 shows the relation between the image brightness and the angle of the polarization filter.

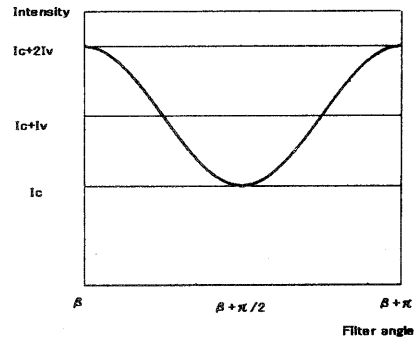


Figure 1: Image brightness plotted as a function of the orientation of a polarization filter

4 Image Acquisition System

The experimental setup for the image acquisition system used in our experiment is illustrated in Figure 2. An object to be modeled in this experiment is placed on the rotary table. A sequence of range images and color images are captured as the object is rotated at a certain angle step. For each rotation step, one range image and thirty five color images, which are taken every five degrees polarization filter rotation in front of the CCD camera, are obtained.

A range image is obtained using a light-stripe range finder with a liquid crystal shutter and a color CCD video camera. Each range image pixel represents an (X, Y, Z) location of a corresponding point on an object surface. The same color camera is used for acquiring range images and color images. Therefore, pixels of the range images and

the color images directly correspond. Color and range images are taken through a polarization filter.

The range finder is calibrated to produce a 3×4 projection matrix Π which represents the translation between the world coordinate system and the image coordinate system. The location of the rotary table is with respect to the world coordinate system is calibrated before image acquisition. Therefore, object location is uniquely determined by the translation matrix T .

A xenon lamp is used as a light source. The lamp is small and placed far enough from the object so that we can assume the lamp is a point light source. In order to illuminate the object with linearly polarized light, a linear polarization filter is placed in front of the lamp.

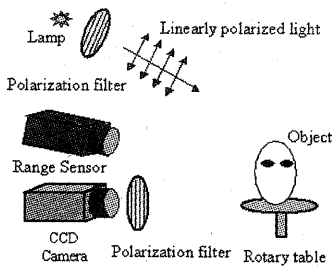


Figure 2: Image acquisition system

5 Separation of Reflection Components

In our experiments, images of a target object are taken every five degrees filter rotation, i.e., 35 images in total. Then, the maximum intensity I_{max} and the minimum intensity I_{min} are determined for every image pixel. Theoretically, only three images are sufficient for determining I_{max} and I_{min} . However, for increasing robustness of estimation of I_{min} and I_{max} , we use more images by rotating the polarization filter.

If $I_{min} - I_{max}$ for a certain pixel is less than a threshold, we consider the pixel to contain only



Figure 3: Input image taken without a polarization filter

the diffuse component. If $I_{max} - I_{min}$ is larger than a threshold value, we consider that the pixel contains the specular component and that $I_{max} - I_{min}$ is equal to $2I_v$ and I_{min} is equal to I_c .

In summary, our separation technique is proceeded as follows. First, a linear polarization filter is placed in front of the light source and camera. Second, input images of an object are captured for every 5 degree rotation of the polarization filter in front of the camera. Third, I_{max} and I_{min} are determined for each pixel. If $I_{max} - I_{min}$ is larger than a threshold value, we determine the pixel contains the specular component and the intensity of the specular component is obtained from $I_{max} - I_{min}$. I_{min} is used for determining the intensity of the diffuse component.

Figure 5 and Figure 4 show an example of reflection component separation by using our proposed method. For comparison, we show another image which were captured without a polarization filter. It shows that the specular and diffuse reflection components were successfully separated even if they have the similar color.

6 Parameters Estimation

After separating the reflection components, we determine the reflection parameters using the separated reflection component images.

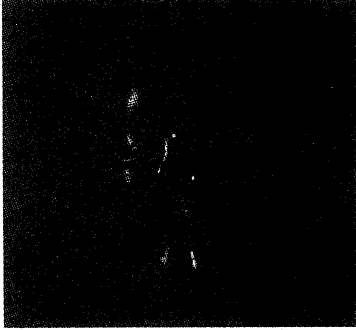


Figure 4: Separated specular component



Figure 5: Separated diffuse component

6.1 Diffuse Parameters estimation

Using the separated diffuse reflection image, we can estimate the diffuse reflection parameters ($I_{D,R}$, $I_{D,G}$, $I_{D,B}$) without undesirable effects from the specular reflection component. The incidence angle θ_i can be obtained by range sensor and camera calibration.

Figure 6 shows the estimated diffuse parameter image. We can see the object surface color which is not attenuated due to the incidence angle.

6.2 Specular Parameters estimation

After estimating the diffuse parameters, we also estimate the specular parameters ($I_{S,R}$, $I_{S,G}$, $I_{S,B}$, σ) using the angle α and the angle θ_r as a known information.

As described in the Section 3, separated specular images are attenuated by a certain ratio de-

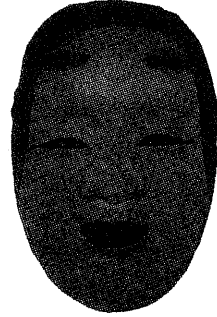


Figure 6: Estimated diffuse parameter image

termined by Fresnel reflection coefficients. But attenuation ratio is constant overall highlight region, we can correctly estimate the specular parameters. More precisely, the Fresnel reflection coefficients are dependent on the incidence angle. However, the Fresnel coefficients are constant around the incidence angle less than 30 degree, and the specular reflection is observed only near the surface normal direction in our experimental setup. Therefore, by setting the light and camera in the same direction, we can assume that the Fresnel reflection coefficients are constant.

There is a significant difference between estimation of the diffuse and specular reflection. Diffuse reflection can be observed overall the object surface where illuminated by a light. On the other hand, specular reflection is observed from a limited viewing direction, and is observed over a narrow area of the object surface. So, we have to select the sampling pixel carefully for specular parameters estimation. We used the same strategy described in [11]. Figure 7 and 8 show the estimated σ and I_S which are projected on the mesh model.

7 Synthesize Images

Using the diffuse and specular reflection parameters estimated in the previous section, and the surface mesh model of the object, we synthesized virtual images of the object under different illumination and viewing conditions. Figure 9 shows

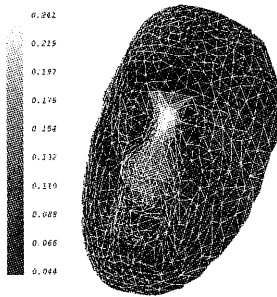


Figure 7: Specular parameter(σ) image

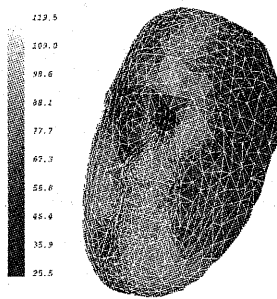


Figure 8: Specular parameter(I_S) image

the comparison between original images and synthesized images viewed from different directions.

8 Conclusion

In this paper, we proposed a new method for separating the reflection components using polarization. Unlike the previously proposed methods, our method does not require the difference of color between the specular reflection and diffuse reflection. So, our method can robustly separate the reflection components even if objects have a white texture and illumination color is white. After reflection components separation, we estimate the parameters of a reflection model by using the separated reflection components. By synthesizing virtual images under the arbitrary illumination and viewing, we have shown that the reflection parameters are successively estimated from the sep-

arated reflection components.

Reference

- [1] K.Ikeuchi and K.Sato, "Determining reflectance properties of an object using range and brightness images," *IEEE Trans. on Pattern Analysis and Machine Intelligence*, vol.13, no. 11, pp.1139-1153, 1991.
- [2] Y.Sato and K.Ikeuchi, "Temporal-color space analysis of reflection," *Journal of Optical Society of America A*, vol.11, no.11, pp.2990-3002, November 1994.
- [3] M.D.Wheeler, Y.Sato, and K. Ikeuchi, "Consensus surfaces for modeling 3D objects from multiple range images," *DARPA Image Understanding Workshop*, 1997.
- [4] L.B.Wolff and T.E.Boult, "Constraining Object Features using a Polarization Reflectance Model," *IEEE Trans. on Pattern Analysis and Machine Intelligence*, Volo.13, No.7, pp.635-657, July 1991.
- [5] T.E.Boult and L.B.Wolff, "Physically based edge labeling," *Proceedings of Computer Vision and Pattern Recognition*, pp.656-663, Maui, Hawaii, June 1991.
- [6] S.K.Nayer, X.Fang, and T.E.Boult, "Removal of specularities using color and polarization," *Proceedings of Computer Vision and Pattern Recognition '93*, pp.583-590, New York City, NY, June 1993.
- [7] S.Shafer, "Using color to separate reflection components," *Color Research and Applications*, Vol.10, pp.210-218, 1985.
- [8] G.J.Klinker, S.A.Shafer, and T.Kanade, "The measurement of highlights in color images," *International Journal of Computer Vision*, Vol.2, No.1, pp.7-32, 1990.
- [9] S.K.Nayer, K.Ikeuchi, T.Kanade, "Surface Reflection: Physical and Geometrical Perspectives," *IEEE Trans. on Patter Analysis and Machine Intelligence*, Vol.13, No.7, pp.611-634, July 1991.
- [10] M. Saito, Y. Sato, K. Ikeuchi, and H. Kashiwagi, "Measurement of surface orientations of transparent object using polarization in highlight," *Journal of Optical Society of America A*, Vol.16, No.9, pp.2286-2293, September 1999.
- [11] Y.Sato, M.D.Wheeler, K.Ikeuchi, "Object Shape and Reflectance Modeling from Observation" *Computer Graphics Proceedings, ACM SIGGRAPH'97*, pp. 379-387, Aug 1997.

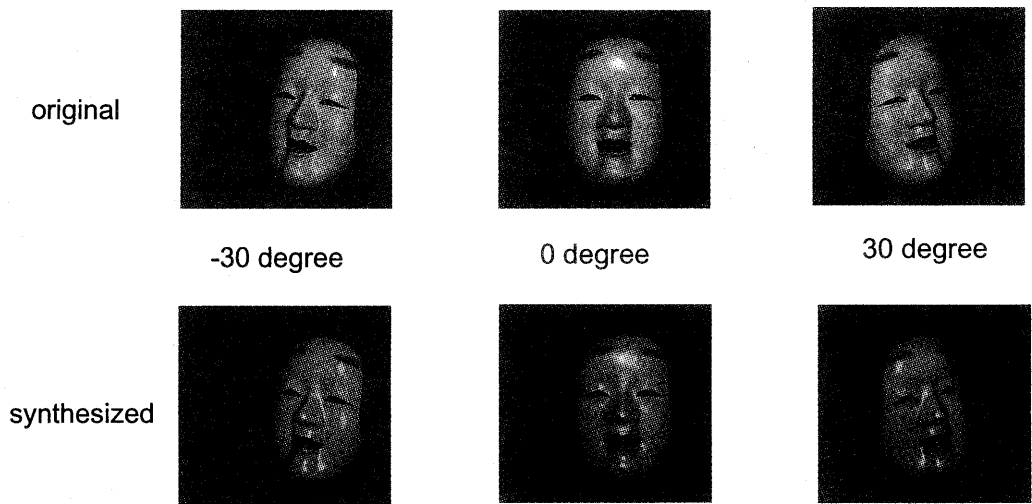


Figure 9: Comparison between input images and synthesized images